# Thalamic and medial prefrontal cortical circuits mediate social defeat stress-induced depression-like behaviors

**Fang Li**
Jinan University
**Hanjie Wang**
Jinan University
**Lianghui Meng**
Jinan University
**Meiying Chen**
Jinan University
**Xuefeng Zheng**
Jinan University
**Yuqing Hui**
Jinan University
**Danlei Liu**
Jinan University
**Yifei Li**
Jinan University
**Keman Xie**
Jinan University
**Jifeng Zhang**
Jinan University
**Guoqing Guo** ( tgqguo@jnu.edu.cn )
Jinan University

---

**Article**

**Keywords:**

**Posted Date:** March 17th, 2022

**DOI:** https://doi.org/10.21203/rs.3.rs-1434398/v1

# Thalamic and medial prefrontal cortical circuits mediate social defeat stress-induced depression-like behaviors

Fang Li [1#], Han-Jie Wang[1#], Liang-Hui Meng[1#], Mei-Ying Chen[1], Xue-Feng Zheng[1], Yu-Qing Hui[1,2], Dan-Lei Liu[1,2], Yi-Fei Li[1], Ke-Man Xie[1], Ji-Feng Zhang[1*] and Guo-Qing Guo[1*]

1 Department of Anatomy, Neuroscience Laboratory for Learning and Memory and Developmental Disorders, Medical College of Jinan University, Guangzhou, China;
2 Department of Gastroenterology, The First Affiliated Hospital, Jinan University, Guangzhou, China;

# Contributed equally.
*Correspondence: Professor Guo-Qing Guo or Professor Ji-Feng Zhang, Department of Anatomy, Neuroscience Laboratory for Learning and Memory and Developmental Disorders, Medical College of Jinan University, Guangzhou, China;
Email: tgqguo@jnu.edu.cn and tzjf_jennifer@jnu.edu.cn

## Abstract

The mediodorsal thalamus (MD) is interconnected with the medial prefrontal cortex (mPFC) and works together to promote some forms of behavioral flexibility. But the relationship between the MD-mPFC circuit and depression is remain unknown. Here, we show that in male susceptible mice, $MD^{GLU}$ neuronal calcium signaling activity is reduced. Chemogenetic inhibition of $MD^{GLU}$ neuronal in male C57BL/J mice resulted in behavioral abnormalities, whereas in susceptible mice, activation of $MD^{GLU}$ neuronal ameliorated depression-like behavior. Brain slice electrophysiology and fiber optic recordings reveal elevated excitability of $mPFC^{GLU}$ neurons in male susceptible mice. Furthermore, we found that in susceptible mice, $mPFC^{GLU}$ neurons exhibited decreased inhibitory postsynaptic currents and unchanged excitatory postsynaptic currents, and increased E/I ratios, whereas activation of $MD^{GLU}$ neurons restored these electrophysiological properties abnormal. Optogenetic activation of the MD-mPFC circuit ameliorates depression-like behaviors in susceptible mice. Taken together, these data demonstrate that the MD-mPFC circuit controls distinct aspects of depression-like behavior.

## Introduction

Depression is a heterogeneous mental disorder characterized by depressed mood, mainly manifested as anhedonia, pessimistic despair, social avoidance, and with or without suicidal behavior (1-3). The underlying neurobiological basis of depression remains elusive owing to the heterogeneity of clinical manifestations and etiologies in patients with depression(4). Extensive neuroimaging literature reports abnormal cortico-striatal-pallidal-thalamic circuits and thalamo-cortical circuit connectivity in patients with depression (5-8). This finding has prompted researchers to further pay attention and study the relationship between the thalamus and depression.

The thalamus is a heterogeneous structure located deep in the brain, and at least two types of thalamic relays have been proposed, “first order thalamic relays” transmit and modulate sensory information from peripheral sensory organs to sensory cortices, and “higher order thalamic relays” can receive input of cortical information and involvement in the regulation of cortico-thalamo-cortical circuits (9-11). As a higher order thalamic relay nucleus, the mediodorsal thalamus (MD) is involved in processing various sensory, emotional, cognitive and behavioral motivations (12-15), suggesting a possible underlying pathological relationship between MD dysfunction and depression. Several studies have shown that MD, as a higher order thalamic relay, can integrate information from limbic nuclei with information from the cortex, and feed this information back to the cortex, especially to the medial prefrontal cortex (mPFC) (13). Anatomical evidence suggests that there is a mutual glutamatergic projection between MD and mPFC, and MD can project to layers II/III and V pyramidal neurons of the mPFC through synaptic transmission, as well as to layer II/III of mPFC PV interneurons (16, 17). Abnormal MD-mPFC connectivity is associated with schizophrenia and cognitive impairment(18, 19). However, the abnormal interconnection between MD and the mPFC and depressive-like behavior is not very clear. In addition, owing to the limitations of human clinical studies, animal models remain a necessary step to explore the pathogenesis of depression. As most depression is related to stressful life events(20-22), to better simulate the pathogenesis of depression caused by social factors, we selected the chronic social defeat stress (CSDS) model to better simulate the pathogenesis of depression caused by social factors.

In this study, we first tested the behavioral performance of mice following CSDS, as well as the number of c-Fos neurons in the MD, and used chemogenetic methods to assess depression-related behaviors following activation or inhibition of MD neurons. Finally, we validated neuronal projections from the MD to the mPFC and determined the role of this MD-mPFC projection in depression-related behavior.

## Results

### Chronic social defeat stress reduces the activation of $MD^{GLU}$ neurons

Stressful stimuli are thought to play an important role in depression, and to clarify the relationship between MD and depression-like behaviors, we employed a chronic social defeat stress (CSDS) model that has long been used to induce depression-like behaviors in animals (Figure S1A). And through social tests, the mice were divided into control, resilient and susceptible groups (Figure S1B-F). In the open field test (OFT), elevated plus maze test (EPM), forced swimming test (FST) and tail suspension test (TST), the susceptible group mice showed obvious depression-like behaviors (Figure S2A-G). In view of the absence of depression-like behaviors in the resilient group, we selected the control group and the susceptible group as our research objects in the following experiments.

First, we performed immediate early gene c-Fos expression mapping in selected control and susceptible mice (Figure 1A, B). We found that the number of neurons activated in the MD was significantly reduced in susceptible mice after exposure to novel aggressive mice compared to controls (Figure 1C). Co-staining with CaMKIIα revealed most of the reductions were in glutamatergic neurons (Figure 1D, E).

Next, we used GCaMP6m, a genetically encoded $Ca^{2+}$ indicator, to examine the effect of novel stressors on the real-time activity of $MD^{Glu}$ neurons during social testing in adult male mice using fiberoptic photometry. First, AAV-mCaMKIIα-GCaMP6m was stereotaxically injected into the MD, and an optical fiber cannula was implanted 0.1 mm above the injection site (Figure 1F). After the virus was expressed, a 5 min social test was performed to record changes in GCaMP fluorescence (Figure 1G). Interestingly, we observed that susceptible mice had much fewer calcium signals in $MD^{Glu}$ neurons than control mice (Figure 1H, I). These data suggest that decreased neuronal activity in patients with MD may be associated with depression.

**Suppression of mouse $MD^{Glu}$ neurons induces behavioral abnormalities in mice**

To test the relationship between $MD^{Glu}$ neurons and depression-like behavior, we silenced these neurons by expressing the inhibitory DREADD receptor, hM4Di. AAV-CaMKIIα-hM4Di-EGFP/AAV-CaMKIIα-EGFP was stereotaxically injected into the MD (Figure 2A, B) and hM4Di was efficiently expressed in CaMKIIα$^{+}$ neurons (Figure 2C). Slice whole-cell recordings confirmed that the application of clozapine-N-oxide (CNO) could effectively reduce the excitability of hM4Di-expressing $MD^{Glu}$ neurons (Figure 2D). CNO was injected intraperitoneally 45min before the behavioral test, and compared to the GFP control group, hM4Di mice spent significantly less time in the center zone during OFT testing (Figure 2E). Similarly, the CNO-injected hM4Di mice spent significantly less time in the open arm during the EPM test (Figure 2F). However, in the forced swimming (Figure 2G) and tail suspension experiments (Figure 2H), there was no significant difference in the immobility time between the control and susceptible groups in the last 4 min. These results suggest that silencing $MD^{Glu}$ neurons induces behavioral disorders in mice.

**Activation of $MD^{Glu}$ neurons reduces depression-like behavior**

To further test the relationship between $MD^{Glu}$ neurons and depression-like behavior, we also applied chemogenetics to activate $MD^{Glu}$ neurons using the excitatory DREADD receptor hM3Dq (Figure 3A), and hM3Dq was efficiently expressed in CAMKIIα$^{+}$ neurons (Figure 3B). In whole cell recordings, we demonstrated that the application of the DREADD agonist CNO effectively increased the excitability of $MD^{Glu}$ neurons in hM3Dq-expressing $MD^{Glu}$ neurons (Figure 3C, D). In freely moving mice, chemogenetic activation by CNO administration restored the center time in the OFT (Figure 3E) and the open-arm time in the EPM (Figure 3F) in susceptible mice as compared with GFP-injected control mice and GFP-injected susceptible mice. Furthermore, activation of $MD^{Glu}$ neurons in susceptible mice reduced post 4 min immobility time in forced swimming (Figure 3G) and tail suspension tests (Figure 3H), indicating that activation of these neurons ameliorated depression-like behavior in mice. The above findings strongly support the hypothesis that MD may be involved in the pathogenesis of depression.

## Increased excitability of $mPFC^{Glu}$ neurons in depression-like states

Previous anatomical evidence has demonstrated interconnections between the MD and the orbitofrontal cortex (OFC), medial prefrontal cortex (mPFC), and granular insular cortex (23-25). While the mPFC is a brain region that is highly correlated with mood, to observe whether the MD-mPFC pathway is related to depression, we first observed the relationship between the mPFC and depression-like behavior. We used the same fiberoptic photometry used to test the MD to examine the effect of novel stressors on the real-time activity of $mPFC^{Glu}$ neurons during social testing in adult male mice. AAV-mCaMKIIα-GCaMP6m was first stereotaxically injected into the mPFC, a fiber-optic cannula was implanted 0.1 mm above the injection site (Figure 4A), and GCaMP6m was efficiently expressed in $CaMKII\alpha^{+}$ neurons (Figure 4B). It was found that GCaMP fluorescence changes in $mPFC^{Glu}$ neurons in susceptible mice were much higher than those in control mice during social testing (Figure 4C-D). Whole-cell recordings from brain slices showed an increase in the spike number of glutamatergic neurons in mPFC layers II/III and V in susceptible mice (Figure 4E-H). These data suggest that $mPFC^{Glu}$ neuronal excitability is enhanced after chronic social defeat stress.

## The MD to mPFC pathway mediates depression-like behaviors

The most striking feature of the thalamus is that it acts as a higher-order relay to interconnect with the cortex and is involved in the occurrence and development of many psychiatric disorders. To elucidate the relationship between MD and mPFC connectivity pathways and depression, we first dissected the functional connectivity of the MD and mPFC using viral tracers. Using brain stereotaxic injection of AAV2/1-Cre virus into the MD and injection of cre-dependent AAV-FLEX-tdTomato virus into the mPFC (Figure 5A), we observed the expression of strong tdTomato fluorescence signal in the mPFC, and these signals could be co-stained with both CaMKIIα, which represents glutamatergic neurons, and GAD67, which represents GABAergic neurons (Figure 5B). To further confirm functional connectivity, we injected the AAV2/2-Retro-Cre virus into the mPFC and cre-dependent AAV-FLEX-tdTomato virus in MD (Figure 5C), where we observed strong tdTomato fluorescence signal expression (Figure 5D). These results demonstrate that MD can project to mPFC and to both glutamatergic and GABAergic neurons in the mPFC. In addition, we injected CTB-555 retrograde tracer virus in mPFC (Figure S3A-C), and we could observe strong red fluorescent signal expression in MD (Figure S3D).

Next, we traced the axons of GFP-labeled MD glutamatergic neurons by injecting chemogenetically activated virus into the MD (Figure 5E) and found that these cells strongly projected to the mPFC (Figure 5F). The electrical activity of mPFC neurons was recorded in whole-cell brain slices, and the results showed that compared with GFP-injected control mice and GFP-injected susceptible mice, the spike number of neurons in hM3dq-injected susceptible mice was significantly improved (Figure 5G).

To further investigate the relationship between the MD and mPFC pathway and depression, we performed optogenetic experiments. We injected AAV2/2-Retro-Cre virus into the mPFC, cre-dependent AAV-DIO-hChR2-EYFP virus or AAV-DIO-EYFP control virus in the MD and implanted a fiber optic cannula 0.1 mm above the injection site (Figure 6A). Efficient ChR2 activation was confirmed using whole-cell recordings from brain slices. By injecting a dynamically changing current into the recorded cells, we found that ChR2-labeled neurons can be driven to fire action potentials at frequencies up to ~30 Hz (Figure 6B). In behavioral experiments, light stimulation activated the MD-mPFC pathway and significantly improved the social interaction ratio in susceptible mice compared to pre-light, but not in susceptible mice injected with the EYFP virus (Figure 6C). In the tail suspension (Figure 6D) and forced swimming tests

(Figure 6E), light stimulation activated the MD-mPFC pathway, and the immobility time after 4 min was significantly reduced compared with susceptible mice injected with EYFP virus.

**CSDS disrupts MD-driven E–I balance in mPFC**

Anatomical studies have demonstrated that MD projects to both glutamatergic and GABAergic neurons in the mPFC, suggesting that MD may have a dual effect on mPFC pyramidal neurons (PNs). Since mPFC pyramidal neuron excitability is elevated in susceptible mice, the activation of $MD^{Glu}$ neurons restores mPFC pyramidal neuron excitability (Figure 5G). Thus, we hypothesized that CSDS resulted in decreased excitatory input to the mPFC by MD, and that the effect might be stronger on GABAergic neurons than on glutamatergic neurons. To test this hypothesis, we recorded miniature excitatory synaptic currents (mEPSCs) from mPFC PNs and found that compared with the control group, the frequency of susceptible mice was reduced and the amplitude was unchanged, whereas the activation of MD glutamate neurons restored the frequency change (Figure 7A-C).

We then recorded miniature inhibitory synaptic currents (mIPSCs) from mPFC PNs and found that the amplitude was smaller in susceptible mice than in control mice, while the frequency did not change, and the amplitude was restored in activated MD glutamate neurons (Figure 7D-F).

To further test this hypothesis, we investigated the effect of CSDS on the excitatory/inhibitory (E/I) balance of the mPFC. We recorded evoked EPSCs and IPSCs from the same pyramidal cells in the mPFC (Figure 7G). Although EPSCs did not change (Figure 7H), IPSC amplitudes were significantly reduced in susceptible mice (Figure 7I), resulting in significantly higher E/I ratios in susceptible mice than in the controls (Figure 7J). However, activation of MD glutamate neurons restored E/I balance. These studies demonstrate that CSDS leads to a decrease in excitatory input to the MD-mPFC, thereby disturbing the mPFC E/I balance and leading to depression-like behaviors.

## Discussion

This study defined the relationship between modulation of the MD-mPFC thalamocortical pathway and depression-like behavior. In a depression model induced by CSDS, MD pyramidal neuron activity was reduced; thus, glutamatergic input from the MD to the mPFC was decreased, mainly manifested as increased mPFC pyramidal neuron excitability, decreased mEPSC frequency, decreased mIPSC and eIPSC amplitudes, and increased E/I ratio. Chemogenetic activation of MD glutamatergic inputs ameliorated mPFC pyramidal neuronal hyperexcitability, mEPSC frequency, mIPSC and eIPSC amplitudes, and E/I balance. In addition to depression-like conditions, chemogenetic or optogenetic activation of MD glutamatergic inputs ameliorates behavioral impairment in mice, highlighting a causal link between functional modulation of the MD-mPFC neural pathway and depression.

First, using fiber-optic recording and chemogenetic approaches, we found that changes in the activity of MD glutamatergic neurons are associated with depression-like behaviors. As a higher order thalamic relay nucleus, the MD is involved in the regulation of the cortico-thalamo-cortical circuit, which means that it can integrate information from the hypothalamus, basal ganglia, olfactory system, amygdala, and cortex, and finally feed back to the cortex(26, 27). It is highly correlated with learning, memory, attention, execution, cognition and emotion(13, 17, 24, 28). Therefore, changes in MD neuronal activity may affect the function of normal cortico-thalamo-cortical circuits and may play an important role in the occurrence of depression. In our study, fiber optic recording and c-Fos staining revealed that the activity of neurons in the MD brain region was reduced in susceptible mice. This finding is consistent with previous imaging findings showing decreased activation of MD in Parkinson's disease (PD) patients with depression (29). In our further study, we found that most of the decreases in the MD brain regions were glutamatergic neurons. Chemogenetically reduces the activity of pyramidal neurons in the MD brain region, and mice exhibited behavioral disturbances in the open field and elevated maze experiments, but did not affect the performance of mice in forced swimming and tail suspension experiments. This phenomenon suggests that other brain regions may be involved in the relationship between MD and depressive-like behaviors. Activation of MD pyramidal neuron activity in susceptible mice rescued depressive behavior. These results suggest that the CSDS-induced depression model may alter MD-related neural pathways.

Second, we combined brain slice electrophysiology, fiber-optic recording, and chemogenetic and optogenetic approaches to determine that MD can affect depression-like behavior in mice by altering afferent modulation of the mPFC. Clinical and basic research has shown that the parafascicular thalamic nucleus (PF), hippocampus, anterior cingulate cortex (ACC), mPFC, lateral habenula (LHb), ventral tegmental area (VTA), hypothalamus, and nucleus accumbens (NAc) are closely related to the pathophysiology of depression (30-34). In depression, the activity of neurons in these regions is affected by dysfunctional regulation of different neural pathways. It is well known that the mPFC is a key brain region related to stress and emotion, and is involved in brain regulation and behavioral disorders in related psychiatric disorders(35-38). Interestingly, in our study, we found that mPFC pyramidal neuron excitability was elevated in susceptible mice using optic fiber recordings and brain slice electrophysiological recordings. Virus tracing results showed that MD can project to the mPFC and simultaneously to the pyramidal neurons and interneurons of the mPFC. Through chemical genetic activation of $MD^{GLU}$ neurons, whole-cell recordings of mPFC PNs revealed that the activation of $MD^{GLU}$ neurons rescued the hyperexcitability of mPFC PNs. This result is also consistent with previous reports that $MD^{GLU}$ neurons project stronger projections to mPFC interneurons than pyramidal neurons in normal anatomy(19, 39). This is also the best explanation for why the decreased glutamatergic projection of MD to the mPFC in susceptible mice results in elevated excitability of mPFC pyramidal neurons. In addition, we specifically activated the MD-mPFC pathway by optogenetic manipulation, and found that activation of the MD-mPFC pathway significantly ameliorated depression-like behaviors in mice.

Finally, we further demonstrated that the key mechanism for the regulation of depression by the MD-mPFC pathway is that MD alters the excitatory and inhibitory balance of the mPFC. Under normal conditions, neurons in the brain maintain a balance between excitation and inhibition, and any mechanism that disrupts this balance can lead to psychiatric disorders(40-42). It has been reported that E/I balance deficits are associated with cognitive function in autism and schizophrenia, and both have GABAergic deficits(18, 43-45). Our results showed that the mEPSC frequency and mIPSC amplitudes in mPFC PNs were reduced in susceptible mice. The same pyramidal neuron-evoked EPSC amplitude did not change in the mPFC, whereas IPSC significantly decreased compared with control mice, resulting in an increased E/I ratio in susceptible mice. This corresponds to a previously validated CSDS-induced increase in the mPFC pyramidal neuron excitability. However, it was again demonstrated that MD glutamatergic neurons provide greater driving force for mPFC interneurons (Figure 8).

Although current studies have revealed that target-cell-dependent regulation of the $MD^{GLU}$-mPFC pathway is associated with increased depression-like behaviors induced by chronic social defeat stress, some important questions remain unanswered.

As previously reported in the literature, MD, as a higher order thalamic relay, can participate in the regulation of the cortical-thalamo-cortical pathway; hence, what are the upstream pathways involved in the regulation of depression-related MD-mPFC? Second, the mPFC has abundant efferent fibers, so where are the downstream target brain regions of the $MD^{GLU}$-mPFC pathway related to depression? Answering these questions will help us to expand our understanding of how coordination between the mPFC and its upstream and downstream brain regions becomes abnormal and contributes to the pathogenesis of depression.

## Methods

### Animals

All experiments were approved by the Animal Care and Use Committee of Jinan University. Adult male C57BL/6J mice (6–8 weeks old) and CD1 (8–9 months old) male mice (Beijing Vital River Laboratory Animal Technology Co., Ltd.) were used. The mice were acclimatized to housing for 1 week under standard conditions. CD-1 mice were kept in a single cage, whereas C57BL/6J mice were housed in groups of five mice per cage with ad libitum access to water and food. They were maintained under a 12/12-h light/dark cycle (lights on from 07:00 to 19:00 daily) at a stable temperature (23 ± 1°C) and humidity (55 ± 10%). Mice were randomly allocated to experimental and control groups. All behavioral experiments were performed during the light phase (09: 00 – 17: 00) unless otherwise specified. The operators were blinded to the experimental group during scoring.

### Chronic social defeat stress (CSDS)

CSDS was performed as described previously(46). Briefly, retired male breeder CD-1 mice were screened for aggressive behavior for 3 consecutive days to validate their aggressiveness profile. Intruder C57BL/6J mice to the home cage of a novel aggressive CD1 mouse for 10 min/day of social defeat stress for 10 consecutive days. After 10 min of social defeat, intruders and residents were separated by a perforated Plexiglass partition into the opposite compartment to maintain sensory contact for the remainder of the 24 h. The experimental mice were singly housed in standard mouse cages after the last defeat session and tested 24 h later for social interactions. Control animals were placed on either side of a perforated divider and rotated daily in a similar manner, unlike the experimental group, which were placed on the other side with normal C57BL/6J mice.

### Social interaction test (SIT)

SIT includes two stages of social interaction tests, each stage is 2.5 min in duration, with an interval of 30s. In the first stage, C57BL/6J mice were placed in an open arena

(42 cm [w] × 42 cm [d] × 42 cm [h]) with an empty wire-mesh cage (10 cm [w] × 6.5 cm [d] × 42 cm [h]). The animals' tracks will be collected in an automated manner by the video-tracking apparatus and software for 2.5 min. The time spent in the interaction zone (8 cm region flanking cage) and in the area opposing the zone (9 cm region along the wall opposing cage) was measured. In the second stage, the target CD-1 mouse was placed within the wire mesh cage, and the measurement method was the same as that in the first stage,

However, the CD-1 aggressor mouse has never been used before. The social interaction ratio was calculated by dividing the time spent in the interaction zone with the second stage by the time spent in the interaction zone with the first stage. Historically, when the index was <1, the animal was considered susceptible, and when the index was > 1, the animal was considered resilient.

**Open field test (OFT)**

The open field chamber (40 × 40 cm) was made of transparent plastic and divided into a 20 × 20 cm center square. Mice were individually placed into the center of the chamber, and the test period lasted for 10 min under dim light conditions using a video-tracking system (TopScanLite Version 2.00). The time the mice spent in the central area was monitored throughout the experiment. The apparatus was cleaned with 75% ethanol and thoroughly dried after each trial.

**Elevated plus maze test (EPM)**

The elevated plus maze apparatus consisted of two closed arms (30 × 5 × 15 cm), two opposing open arms (30 × 5 cm) and a central platform (5cm× 5cm). The maze was elevated to 50 cm above the floor. The test mice were placed on the center platform facing an open arm and allowed to freely explore the maze for 10 min to monitor their behaviors. The time spent in the open arms and number of entries into the open arms were analyzed using a video-tracking system (TopScanLite Version 2.00). The apparatus was cleaned with 75% ethanol and thoroughly dried after each trial.

**Forced swimming test (FST)**

The test mice were placed individually in a cylinder (28-cm height, 16-cm internal diameter) containing fresh water (22～24 ℃, 20-cm depth) and forced to swim for 6 min (47). The last 4 min of immobile timewas recorded using a video-tracking system (TopScanLite version 2.00). Clear water was used as a replacement for both animals. Immobility was defined as floating in the water without struggling or just making the necessary light movements to avoid drowning. After the test, the mice were wiped dry and returned to their home cage.

**Tail-suspension test (TST)**

The tail suspension experiment is a classic experiment used to evaluate depression-like behaviors in animals. Briefly, the test mice were suspended by their tails with adhesive tape (1 cm from the tail tip) approximately 50 cm above the floor for 6 min (48, 49). When the mouse is suspended in a high place, it immediately shows escape-like behavior, and then becomes passive and immobile. The immobile time during the last 4 min of the 6-min test period was recorded using a video tracking system (TopScanLite Version 2.00).

**Quantification of c-Fos immunostaining**

To observe the changes in neuronal activity of MD brain regions in depression mice, we first performed a 10-day CSDS test in C57 mice, and performed a social interaction test 24 h later. The control and CSDS groups were anesthetized and infused to collect the brain after 90min of social testing, followed by post-fixation with 4% paraformaldehyde (PFA) and cryoprotection using 15% and 30% of sucrose overnight. Cryostat sections of the mouse brains on a Leica cryostat (Leica CM1900) were subjected to immunostaining for c-Fos. In brief, brain sections were washed three times with 0.01M phosphate-buffered saline (PBS) and blocked for 1 h in PBS (containing 5% bovine serum albumin with 1% Triton-X) at room temperature and followed by incubation with the appropriate antibody (rabbit anti-Fos 1:500, #2250s, Cell Signaling Technology, CST) overnight at 4℃. Next, the slides were washed three times with PBS for 10 min each time and incubated with the appropriate secondary antibody (Alexa 488-conjugated goat anti-rabbit, 1:1500, #A21206, Invitrogen), overnight at 4℃, and washed for an additional three times in PBS, thereafter. Finally, the slides were blocked with blocking fluid containing DIPA (#17985-50, Electron Microscopy Sciences EMS) to prevent fluorescence quenching. The immunofluorescence labeling method for CaMKIIα (Mouse anti-CaMKIIα 1:400, #Ab5683, Abcam) and GAD67 (mouse anti-GAD67 1:500, # ab26116, Abcam) was the same as above, and the corresponding secondary antibody was: goat anti-mouse antibody (1:1500, #A31570, Invitrogen). In each mouse, the number of c-Fos-labeled neurons per unit area was calculated from four consecutive brain slices (30 μm /slice) of MD.

**Virus and trace injection**

Mice were anesthetized with 0.5% pentobarbital sodium, (50 mg/kg, i.p.) and fixed using a stereotaxic instrument (RWD, Shenzhen, China). Erythromycin eye ointment was applied to prevent the cornea of the mice from drying. The skin was cut to expose the dura and the virus was bilaterally injected into the MD or mPFC using calibrated glass microelectrodes connected to a microinjection syringe. We used an infusion pump (KD Scientific Legato, USA) to inject 300 nL of virus into each area at a rate of 50 nL/min, and then removed the syringe 10 min later to allow diffusion of the virus at the injection site and then slowly withdrawn.

For monosynaptic anterograde tracing of MD-mPFC, 300 nL helper virus AAV2/1-hsyn-Cre-WPRE-pA (AAV- hsyn-Cre, $5 \times 10^{12}$ vg $ml^{-1}$, Shanghai Taitool Bioscience Co., Ltd, S0278-1-H5) was injected into the MD (AP: −0.7 mm; ML: ±0.31 mm; DV: −3.35 mm) of C57 mice. Simultaneously, 300 nl of AAV2/9-hSyn-FLEX-tdTomato-T2A-WPRE-PA (AAV-FLEX-tdTomato, $5 \times 10^{12}$ vg $ml^{-1}$, Shanghai Taitool Bioscience Co., Ltd, S0161-9) was injected into the mPFC (AP: +2.2 mm; ML: ±0.33 mm; DV: -2.3 mm). Three weeks after virus injection, mice were anesthetized and transcardially perfused. Brain slices were used to track tdTomato signals and for co-staining with mCaMKIIα-specific or GAD67-specific antibodies in the mPFC.

For retrograde monosynaptic tracing MD-mPFC, 300 nL helper viruses AAV2/2-

Retro-hSyn-Cre-WPRE-pA (AAV2/2-Retro-Cre, 5 × $10^{12}$ vg $ml^{-1}$, Shanghai Taitool Bioscience Co., Ltd, S0278-2R) was injected into the mPFC of C57 mice. Simultaneously, 300 nl of AAV2/9-hSyn-FLEX-tdTomato-T2A-WPRE-PA (AAV-FLEX-tdTomato, 5×$10^{12}$ vg $ml^{-1}$, Shanghai Taitool Bioscience Co., Ltd, S0161-9) was injected into the MD. Three weeks after virus injection, the mice were anesthetized and transcardially perfused. Brain slices were used to track the tdTomato signals. Another strategy is to inject 300 nL of cholera toxin subunit B, CTB-555 (1 μg/μl, 300 nL, Wuhan Brain VTA, CTB-02) into the PFC. Ten days after virus injection, mice were anesthetized and transcardially perfused. Brain slices were used to track the CTB-555 signal.

For calcium imaging manipulation, the AAV2/9-mCaMKIIα-GCaMP6m-WPRE-pA (AAV-mCaMKIIα-GCaMP6m, 1 × $10^{13}$ vg $ml^{-1}$, 200 nL, Shanghai Taitool Bioscience Co., Ltd, S0481-9-H5) was delivered into the MD or mPFC of control and CSDS mice.

For chemogenetic manipulation, the AAV2/9-CaMKIIα-hM3D(Gq)-EGFP-WPRE-pA (AA-CaMKIIα-hM3Dq-EGFP, 3.2×$10^{12}$ vg $mL^{-1}$, 300nL, Wuhan Brain VTA, PT-0525) or AAV2/9-CaMKIIα-hM4D(Gi)-EGFP-WPRE-hGHpA (AAV-CaMKIIα-hM4Di-EGFP, 3.2×$10^{12}$ vg $mL^{-1}$, 300nL, Wuhan Brain VTA, PT-0524) virus was injected into the MD. The AAV2/9-CAMKIIα-EGFP-WPRE-hGHpA (AAV-CaMKIIα-EGFP, 3.2 × $10^{12}$ vg $mL^{-1}$, 300nL, Wuhan Brain VTA, PT-0290) were used as the control virus. Three weeks after the viral injection, an intraperitoneal injection of CNO (3.3 mg/kg, Sigma) was administered 45 min before the behavioral tests.

For optogenetic manipulation, the helper virus AAV2/2-Retro-hSyn-Cre-WPRE-pA (AAV2/2-Retro-Cre, 3.3×$10^{12}$ vg $mL^{-1}$, Shanghai Taitool Bioscience Co., Ltd, S0278-2R) was injected into the mPFC of CSDS mice. Simultaneously, the Cre-dependent virus AAV2/9-hEF1a-DIO-hChR2(H134R)-EYFP-WPRE-pA (AAV-DIO-hChR2-EYFP, 3.3 × $10^{12}$ vg $mL^{-1}$, 200nL, Shanghai Taitool Bioscience Co., Ltd, S0199-9-H50) virus or AAV2/9-hEF1a-DIO-EYFP-WPRE-pA (AAV-DIO-EYFP, 3.3 × $10^{12}$ vg $mL^{-1}$, 200nL, Shanghai Taitool Bioscience Co., Ltd, S0196-9-H20) virus was injected into the MD of CSDS mice.

For the above sections, only mice with the correct injection site were included in the data analysis.

## Fiber Photometry

To investigate the relationship of the MD or mPFC with depression-like behavior, Optical fibers (200 μm O.D., 0.37 NA, Inper, Hangzhou, China) housed in a ceramic ferrule were implanted 0.1 mm above the injection site. Fluorescence signals were recorded using an intelligent fiber photometry system (470 nm, Inper, Hangzhou, China). For recordings of MD or mPFC pyramidal neuron activity during social interaction, test mice were individually placed into an open-field apparatus in the presence of a novel CD1 mouse in the cage for 5 min. At the end of the experiment, the positions of the virus and optical fiber were evaluated. The photometry data were exported from CamFiberPhotometry to MATLAB mat files for further analysis. The data were segmented according to behavioral events within individual trials. The fluorescence change ($\Delta F/F$) was calculated using $(F-F0)/F0$, which were presented as heatmaps or average plots.

## In vivo optogenetic manipulations

To investigate the relationship between MD and mPFC and depression-like behavior, mice were first anesthetized and placed on a stereotaxic apparatus, and an optical fiber cannula was implanted into the MD. Dental cement and screws were used to secure the optical fiber cannula to the skull of the mouse. The optical fiber was connected to an intelligent optogenetic system (Inper, B1-465, Hangzhou, China) using an optical fiber cannula to deliver a 5 ms pulse of blue light (465 nm, 10 mW, 30Hz). At the end of the experiment, the position of the optical fiber was assessed, and the data from the mice that failed to implant the optical fiber were deleted.

## Whole-cell patch clamp recordings

Coronal slices from the mPFC (300 μm thick) were prepared using a fully automatic vibrating slicer (Leica VT1200 S) in an ice-cold dissection buffer. Brain slices were immediately transferred to artificial cerebrospinal fluid (ACSF) containing the following (in mM): 26 $NaHCO_3$, 3 KCl, 1.25 $NaH_2PO_4$, 10 dextrose, 124 NaCl, 1 $MgCl_2$, and 2 $CaCl_2$, bubbled with 95% $O_2$/5% $CO_2$ at 34°C for 30 min. After 30 min, the brain slices were placed at room temperature until recording. Pyramidal cells in the mPFC areas were visualized using a water-immersion objective (×40) with depth correction on an upright microscope (Nikon Eclipse FN1, Japan) equipped with interference contrast (IR/DIC) and an infrared camera connected to the video monitor. Data were acquired after low-pass filtering at 2 kHz and digitized at 10 kHz using a Sutter amplifier. The series resistance (Rs) was < 30 MΩ and an input resistance > 100 MΩ was studied.

To examine the gamma-aminobutyric acid (GABA) receptor-mediated mIPSCs from pyramidal cells in the mPFC, ACSF was perfused with 1 μM TTX (sodium channel blocker), 20 μM CNQX (AMPA receptor blocker), and 100 μM D, L-APV (NMDA receptor blocker). The mIPSCs were recorded in voltage -clamp mode (holding at –60 mV) using pipettes (3–5 MΩ) filled with Cs-based internal solution consisting of the following (in mM): 120 CsCl, 0.2 $CaCl_2$, 8 NaCl, 2 EGTA, 10 HEPES, 5 QX-314, 4 ATP, and 0.5 GTP, pH 7.2–7.4, osmolality of 300 mOsm/kg.

To measure the excitatory-inhibitory (E/I) current ratio, cells were first clamped at the reversal potential of $GABA_A$ receptors (–65 mV) to evoke the maximal amplitude of EPSCs in response to at least 15 stimulus intensities and then switched to the reversal potential of AMPA/NMDA receptors (+5 mV) to evoke the maximum amplitude of IPSCs. Finally, the maximum of the 15 responses was averaged to obtain the E/I ratio. Patch pipettes (2–5 MΩ) were filled with the internal solution consisting of the following (in mM): 130 $CsMeSO_3H$, 10 HEPES, 3 lidocaine *N*-ethyl bromide (QX-314), 0.2 EGTA, 4 ATP, 0.5 GTP, 10 Na-phosphocreatine, pH 7.2–7.4, and osmolality of 300 mOsm/kg.

Current-evoked firing was recorded in current-clamp mode (dynamic holding at -70mV). Patch pipettes (2–5 MΩ) were filled with an internal solution consisting of the following (in mM): 130 potassium gluconate, 130 K-gluconate, 10 KCl, 10 HEPES, 0.2 EGTA, 0.5 GTP, 4 ATP, and 10 Na-phosphocreatine, with a pH of 7.2–7.4 and osmolality of 300 mOsm/kg.

**Statistics and reproducibility**

All statistics are presented as the mean ± SEM in this work. Data analysis was performed using the GraphPad Prism 9.2 software (GraphPad Software, San Diego, CA, USA). Specific statistical analysis methods including sample size, can be found in the figure legends. Student's *t*-tests were used for comparisons between two groups, one-way analysis of variance was used to compare three groups with one factor and two-way analysis of variance for two-factor experimental data. Significance levels are shown as * $p < 0.05$, ** $p < 0.01$, *** $p < 0.001$, and not significant (NS). The data recorded by electrophysiology were analyzed offline using the SutterPatch software.

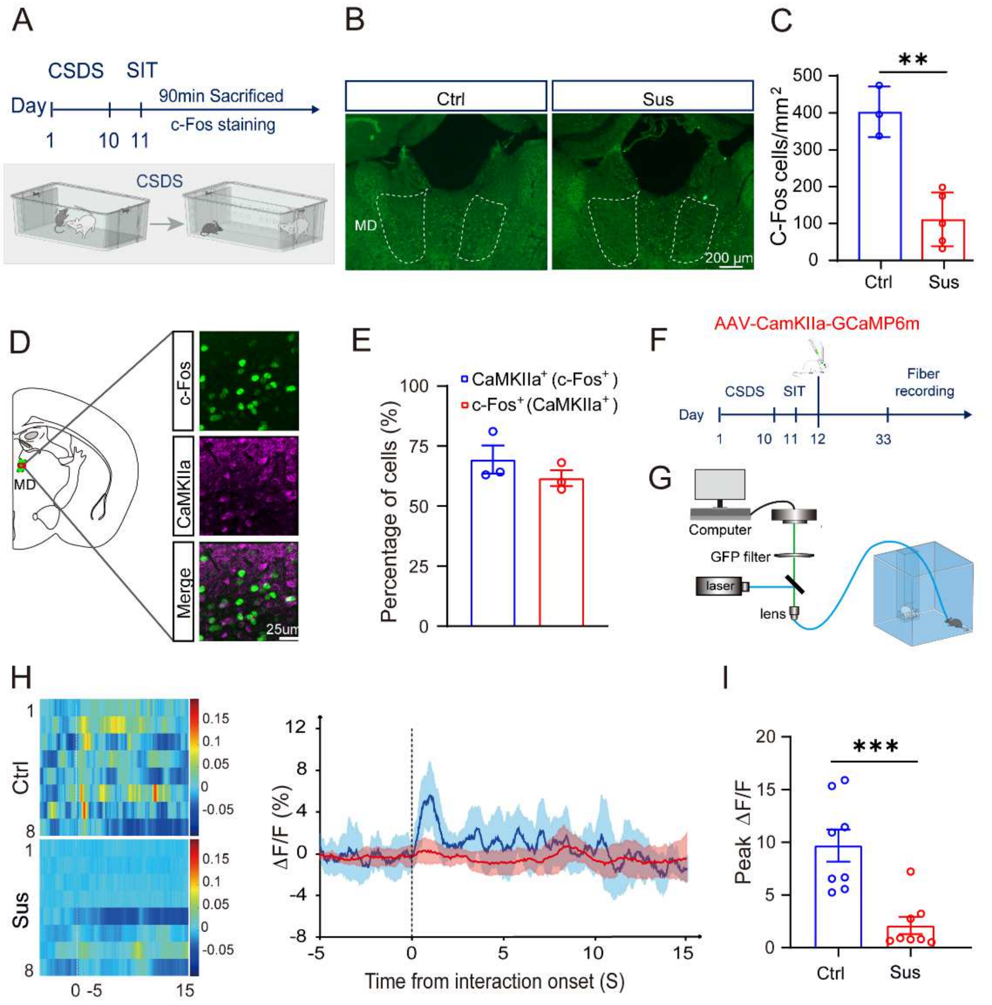


**Figure 1. MD$^{GLU}$ neurons activity is reduced by Chronic social defeat stress.**

**(A).** Experimental schedule of c-Fos staining in MD brain regions. **(B).** Representative confocal images of c-Fos staining in the MD for Ctrl and Sus experimental animals. Scale bar = 200µm. **(C).** Quantification of the number of c-Fos + neurons in the MD for each treatment (Ctrl, n = 3 mice; Sus, n = 5 mice;) **(D).** Representative images showing colocalization of c-Fos (green) and CaMKIIα (Purple) signals. **(E).** Quantification of the percentage of CaMKIIα+ cells in the c-Fos+ population (blue) and the percentage of c-Fos+ cells in the CaMKIIα+ population (red). **(F, G).** Experimental schedule and experimental setup for optical fiber recording in MD. **(H).** Heatmap of calcium signals in MD neurons elicited by social interaction. **(I).** Quantification of social test-induced peak ΔF/F (%) for Ctrl and Sus mice (Ctrl, n = 8 mice; Sus, n = 8 mice;). CSDS, chronic social defeat stress; SIT, social interaction test; MD, mediodorsal thalamus; Ctrl, control; Sus, susceptible. **p＜0.01, ***p＜0.001, Unpaired Student's t test; Data represents mean ± SEM.

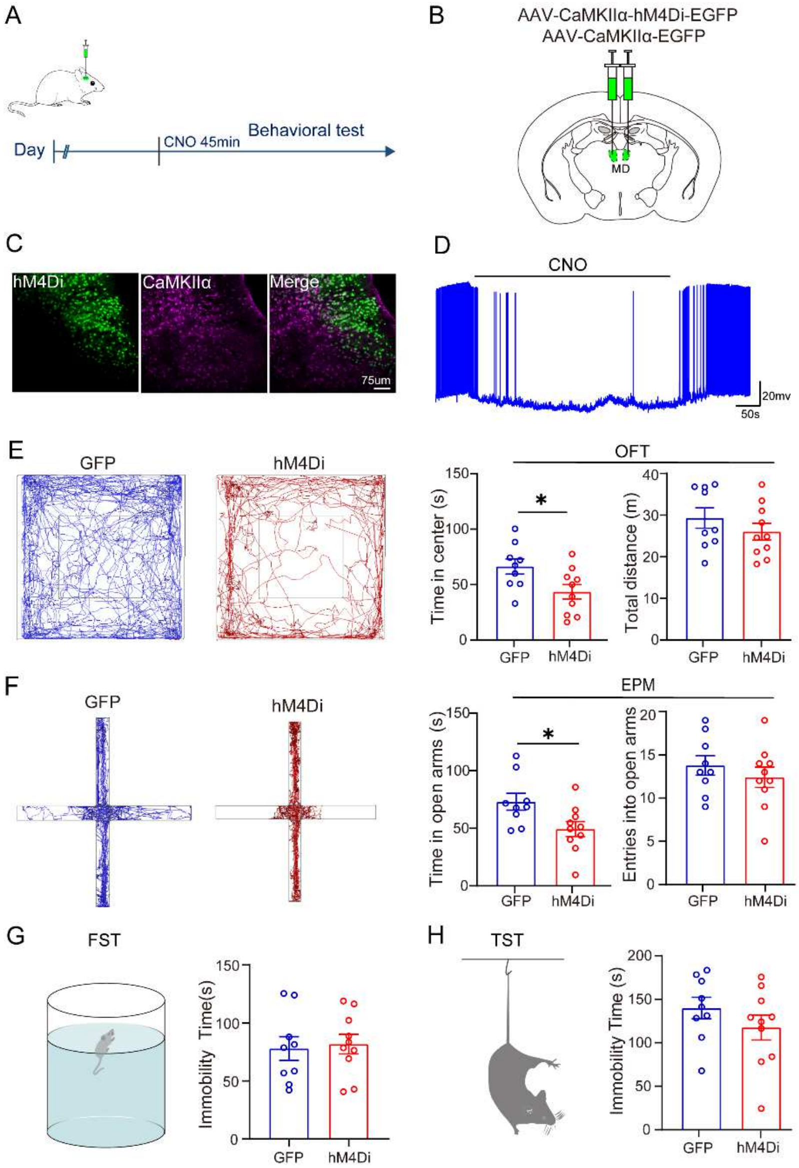


**Figure 2. Silencing $MD^{Glu}$ neurons enhances behavioral abnormalities in mice.**

**(A).** Behavioral testing schedule after chemical genetic inhibition of virus injection. **(B).** Schematic diagram of the location of chemical genetic inhibition of virus injection. **(C).** hM4Di (reflected by EGFP expression in AAV-CaMKIIα-hM4Di-EGFP) co-stained with CaMKIIα (Purple). Scale bar = 75μm. **(D).** MD neurons expressing hM4Di can be inhibited by bath application of CNO (10μM). **(E).** Left: representative locomotion tracking of mice expressing GFP control virus and hM4Di experimental virus in OFT. Right: quantification of center time and total distance in the OFT. **(F).** Left: representative locomotion tracking of mice expressing GFP control virus and hM4Di experimental virus in EPM. Right: Quantify the time and number of mouse entry into the open arm in the EPM test. **(G).** Quantify post-4min immobility time in the FST test. **(H).** Quantify post-4min immobility time in the TST test. GFP, n = 9 mice; hM4Di, n = 10 mice; GFP: mice that received MD injection of AAV-CaMKIIα-EGFP and i.p. injection of CNO (3.3 mg/kg); hM4Di: mice that received MD injection of AAV-CaMKIIα-hM4Di-EGFP and i.p. injection of CNO (3.3 mg/kg). MD, mediodorsal thalamus; CNO, Clozapine-N-oxide; OFT, open field test; EPM, elevated plus maze test; FST, forced swim test; TST, tail suspension test. *$p < 0.05$, Unpaired Student's t test; Data represent mean ± SEM.

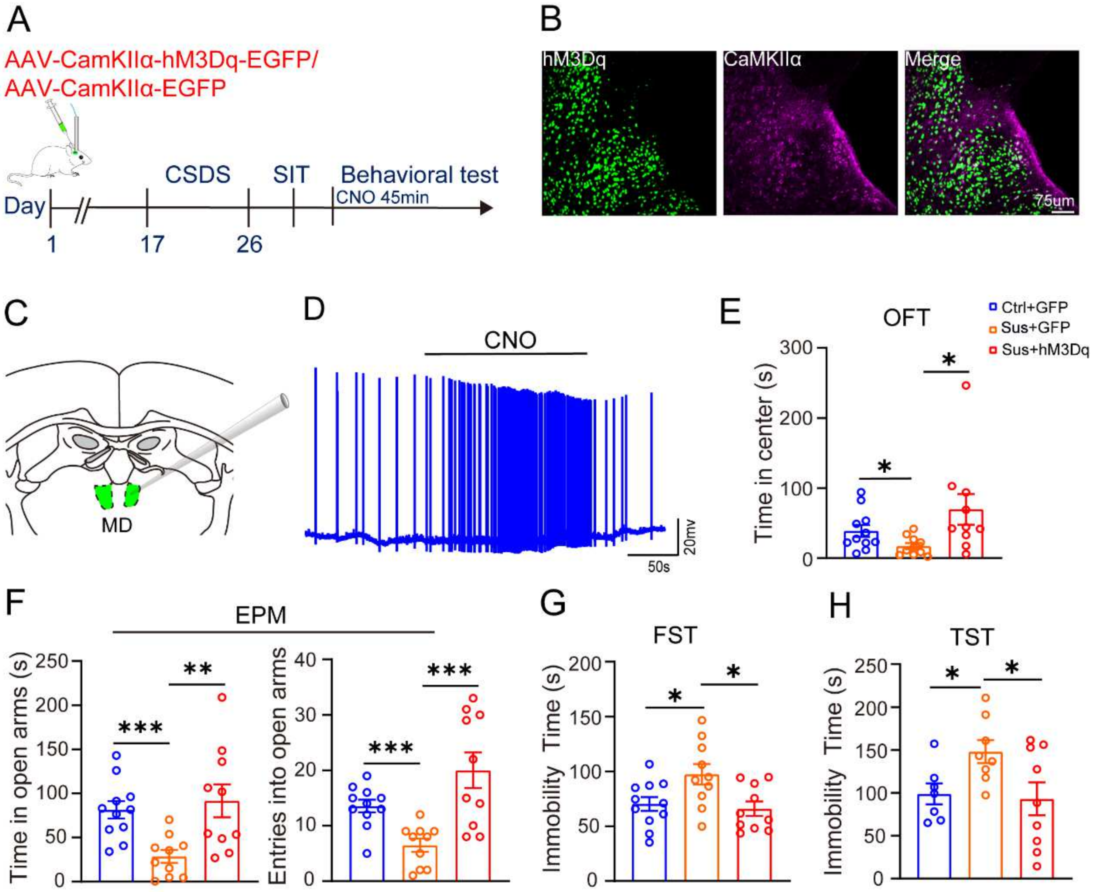


**Figure 3. Activation of $MD^{Glu}$ neurons alleviates depression-like behavior.**

**(A).** Timeline of behavioral testing following chemical genetic activation of virus injection. **(B).** hM3Dq (reflected by EGFP expression in AAV-CaMKIIα-hM3Dq-EGFP) co-stained with CaMKIIα (Purple). Scale bar = 75μm. **(C).** Schematic diagram of the location of whole-cell patch-clamp recordings. **(D).** MD neurons expressing hM3Dq can be activated by bath application of CNO (10μM). **(E).** Quantification of center time in the OFT (Ctrl+GFP, n = 11 mice; Sus+GFP, n = 10 mice; Sus+hM3Dq, n = 10 mice;).

**(F).** Quantify the time and number of mouse entry into the open arm in the EPM test (Ctrl+GFP, n = 11 mice; Sus +GFP, n = 10 mice; Sus +hM3Dq, n = 10mice;). **(G).** Quantify post-4min immobility time in the FST test (Ctrl+GFP, n = 11 mice; Sus+GFP, n = 10 mice; Sus+hM3Dq, n = 10mice;). **(H).** Quantify post-4min immobility time in the TST test (Ctrl+GFP, n = 7 mice; Sus+GFP, n = 8 mice; Sus+hM3Dq, n = 9 mice;).

Ctrl+GFP: Control mice that received MD injection of AAV-CaMKIIα-EGFP and i.p. injection of CNO (3.3 mg/kg); Sus+GFP: Sus mice that received MD injection of AAV-CaMKIIα-EGFP and i.p. injection of CNO (3.3 mg/kg); Sus+hM3Dq: Sus mice that received MD injection of AAV-CaMKIIα-hM3Dq-EGFP and i.p. injection of CNO (3.3 mg/kg). CSDS, chronic social defeat stress; SIT, social interaction test; MD, mediodorsal thalamus; Ctrl, control; Sus, susceptible. OFT, open field test; EPM, elevated plus maze test; FST, forced swim test; TST, tail suspension test. *$p < 0.05$, **$p < 0.01$, ***$p < 0.001$, One-way ANOVA test (E-H); Data represent mean ± SEM.

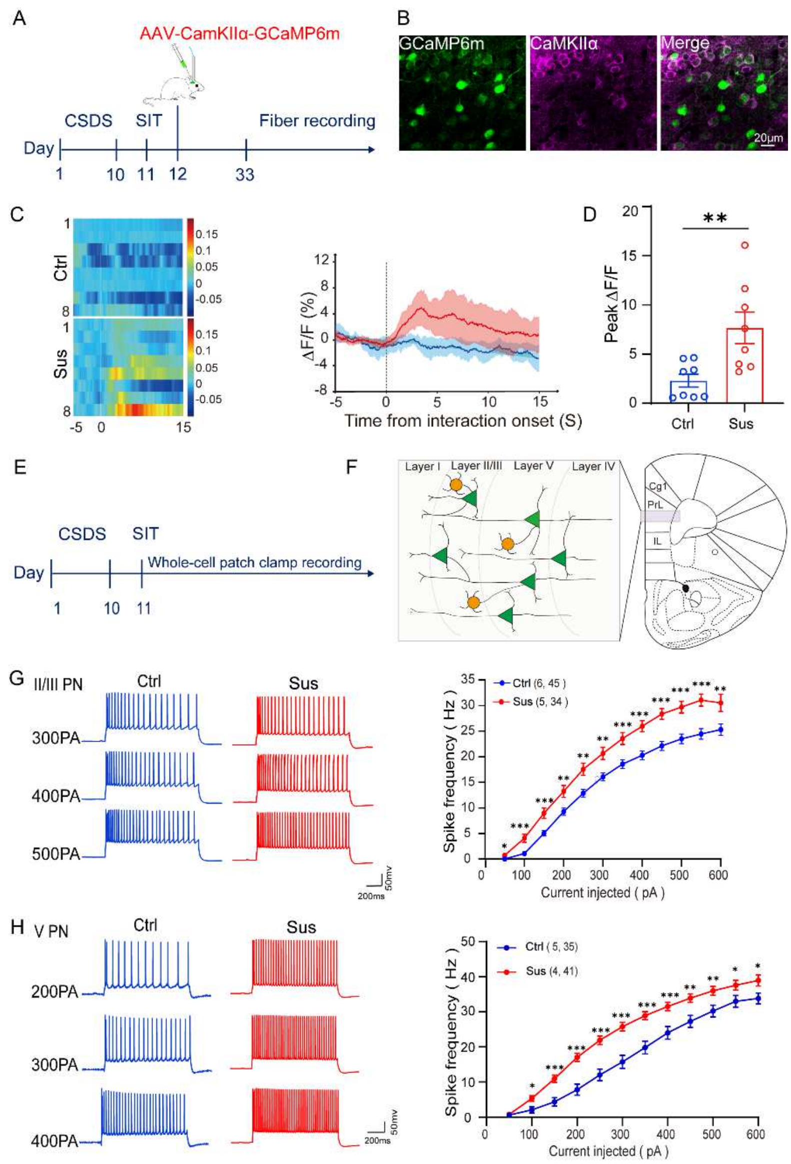


**Figure 4. mPFC glutamatergic neurons are activated by chronic social defeat stress.**

**(A).** Timeline of mPFC calcium signal detection. **(B).** GCaMP6m (reflected by EGFP) co-stained with CaMKIIα (Purple). Scale bar = 20μm. **(C).** Heatmap of calcium signals in mPFC neurons elicited by social interaction. **(D).** Quantification of social test-induced peak ΔF/F (%) for Ctrl and Sus mice (Ctrl, n = 8 mice; Sus, n = 8 mice;). **(E).** Brain slices electrophysiological recording timeline. **(F).** Schematic diagram of mPFC anatomy. **(G)** and **(H).** Action potential data from mPFC layers II/III and V PNs showing that neuronal activity is increased in Sus mice compared with Ctrl mice (G：Ctrl, n = 45 cells from 6 mice, Sus, n=34 cells from 5 mice; H: Ctrl, n = 35 cells from 5 mice, Sus, n=41 cells from 4 mice;). mPFC, medial prefrontal cortex; CSDS, chronic social defeat stress; SIT, social interaction test; Ctrl, control; Sus, susceptible. PNs, Pyramidal neurons; *P < 0.05, **p＜0.01, ***p＜0.001, Unpaired Student's t test (D) or Two-way ANOVA test (G and H); Data represents mean±SEM.

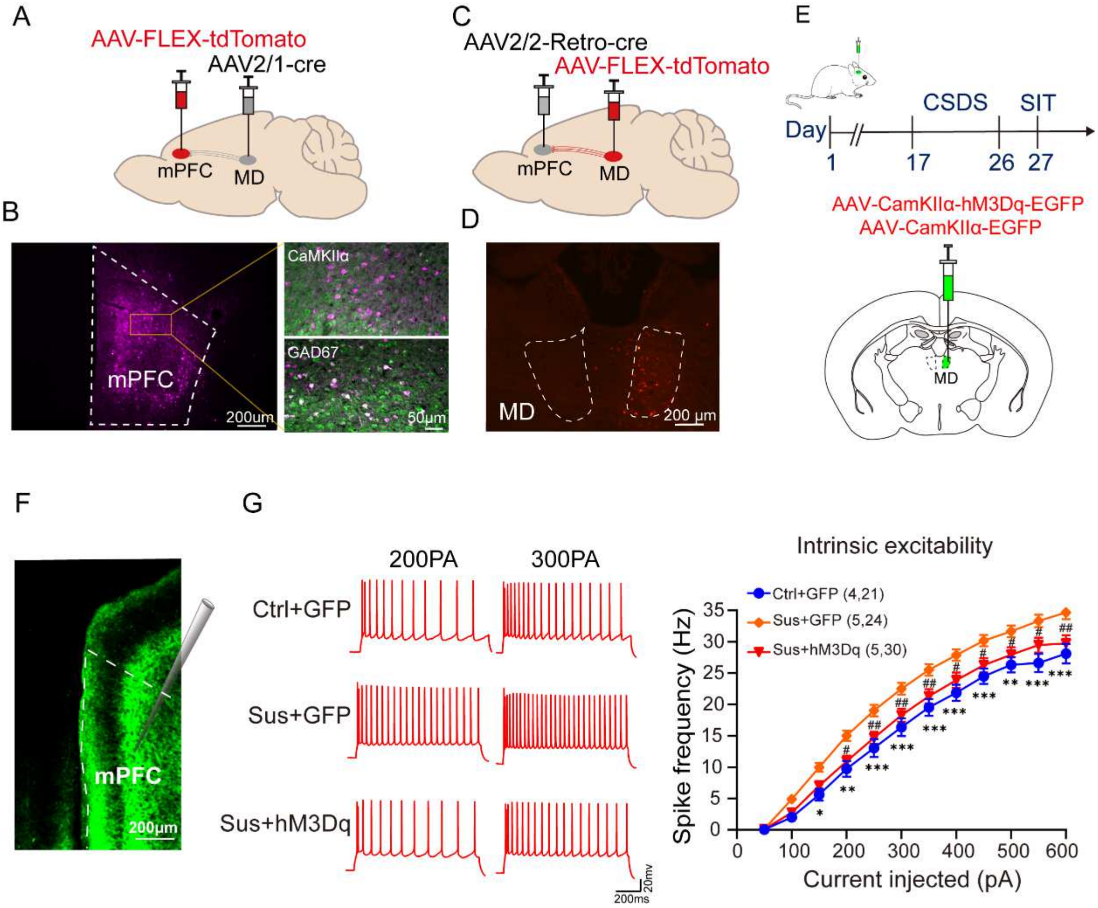


**Figure 5. Activation of MD$^{Glu}$ neurons reduces the increase in intrinsic excitability of mPFC pyramidal neurons induced by CSDS.**

**(A).** Schematic of MD injection of AAV2/1-Cre and mPFC injection of AAV-FLEX-tdTomato into C57BL/J mice. **(B).** Representative image of tdTomato+ fibers (Purple) in C57BL/J mouse with MD injection of AAV2/1-Cre and mPFC injection of AAV-FLEX-tdTomato. Scale bar = 200μm. Right: tdTomato (reflected by AAV-FLEX-tdTomato, Purple) co-stained with CaMKIIα (green) and GAD67 (green). Scale bar = 50μm. **(C).** Schematic of MD injection of AAV-FLEX-tdTomato and mPFC injection of AAV2/2-Retro-Cre into C57BL/J mice. **(D).** Representative image of tdTomato+ fibers in C57BL/J mouse with MD injection of AAV-FLEX-tdTomato and mPFC injection of AAV2/2-Retro-Cre. Scale bar =200μm. **(E).** Schematic illustration of MD chemical genetic activation of virus injection. **(F).** Representative images of mPFC EGFP+ fibers in C57BL/J mice, MD injected with AAV-CaMKIIα-hM3Dq-EGFP or AAV-CaMKIIα-EGFP. Scale bar = 200μm. **(G).** Action potential data from mPFC layer V PNs showed increased neuronal activity in Sus mice compared to ctrl mice, and activation of MD$^{GLU}$ neurons restored electrical activity in mPFC PNs. mPFC, medial prefrontal cortex; MD, mediodorsal thalamus; CSDS, chronic social defeat stress; SIT, social interaction test; Ctrl, control; Sus, susceptible. PNs, pyramidal neurons. Ctrl+GFP: Control mice that received MD injection of AAV-CaMKIIα-EGFP and CNO bath applications (10μM); Sus+GFP: Sus mice that received MD injection of AAV-CaMKIIα-EGFP and CNO bath applications (10μM); Sus+hM3Dq: Sus mice that received MD injection of AAV-CaMKIIα-hM3Dq-EGFP and CNO bath applications (10μM). *$P < 0.05$, **$p < 0.01$, ***$p < 0.001$, Two-way ANOVA test (G); Data represents mean ± SEM.

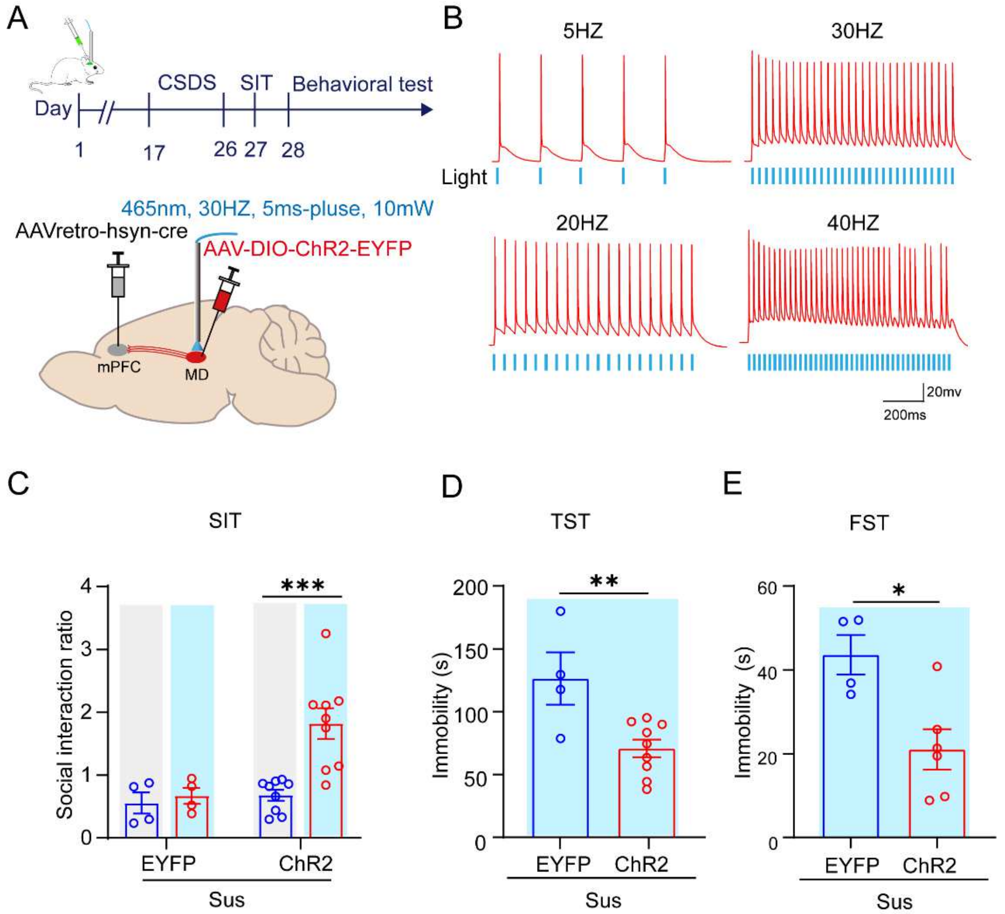


.

**Figure 6. The MD-mPFC circuit controls depression-like behaviors induced by CSDS.**

**(A).** Schematic diagram of optogenetic virus injection (MD injection of AAV-DIO-ChR2-EYFP and mPFC injection of AAVretro-hsyn-Cre into C57BL/J mice) and timeline of behavioral testing. **(B).** Example traces of action potentials of a recorded MD EYFP+ neuron in response to pulses of blue light at 5, 20,30 and 40 Hz. **(C).** Quantification of social interaction ratio. EYFP (left, n = 4) and ChR2 expressing (right, n = 9) Sus mice in LED-off (gray) and LED-on (Blue) conditions. **(D).** Quantify post-4min immobility time in the TST test with LED-on (Sus+EYFP, n = 4 mice; Sus+ChR2, n = 9 mice). **(E).** Quantify post-4min immobility time in the FST test with LED-on (Sus+EYFP, n = 4 mice; Sus+ChR2, n = 6 mice). mPFC, medial prefrontal cortex; MD, mediodorsal thalamus; CSDS, chronic social defeat stress; SIT, social interaction test; FST, forced swim test; TST, tail suspension test; Sus, susceptible. Sus+EYFP: Sus mice that received MD injection of AAV-DIO-EYFP and mPFC injection of AAVretro-hsyn-Cre; Sus+ChR2: Sus mice that received MD injection of AAV-DIO-ChR2-EYFP and mPFC injection of AAVretro-hsyn-Cre. *$p < 0.05$, ***$p < 0.001$, Two-way ANOVA test (C); Unpaired Student's t test (D,E); Data represent mean ± SEM.

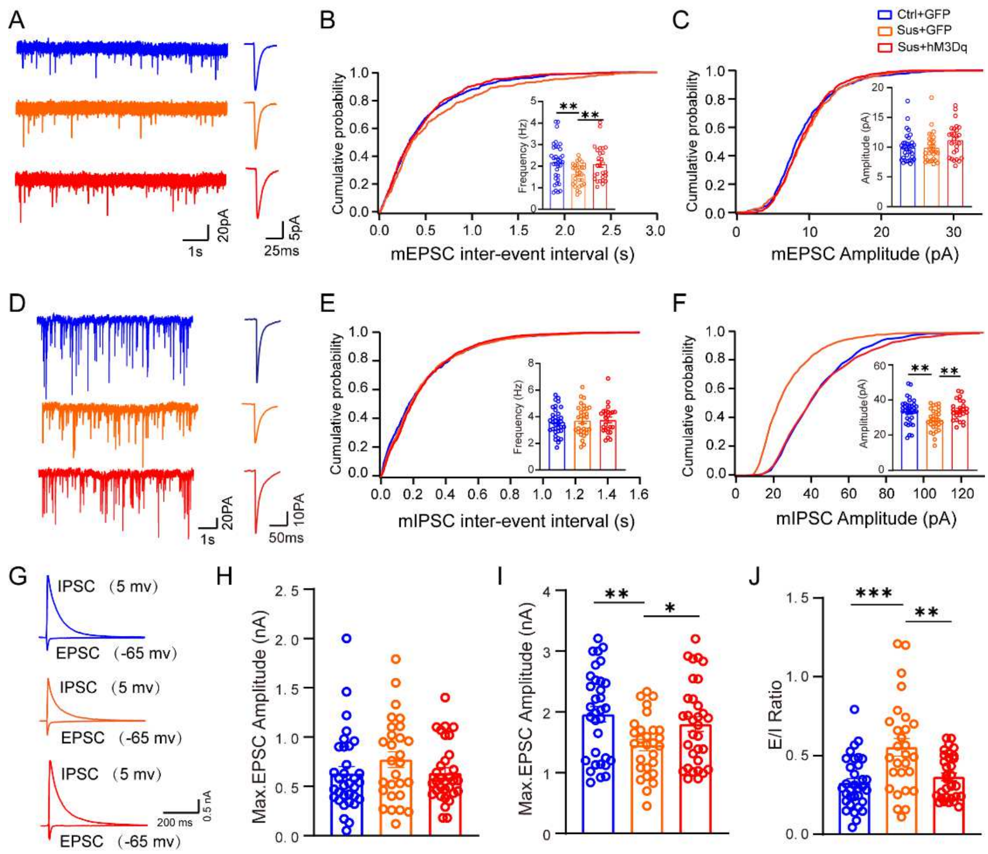


# Figure 7. CSDS impairs synaptic transmission from MD to mPFC.

**(A).** Representative (left) and average (right) traces of mEPSCs recorded from CtrL+GFP (blue), Sus+GFP (orange) and Sus+hM3Dq (red) mouse mPFC PNs. **(B and C).** Cumulative probability of mEPSC inter-event interval (Left) and amplitude (Right) in CtrL+GFP (blue, n = 35 cells from 3 mice), Sus+GFP (orange, n = 29 cells from 3 mice) and Sus+hM3Dq (red, n = 26 cells from 3 mice) groups. Insets: average mEPSC frequency and amplitude from CtrL+GFP, Sus+GFP and Sus+hM3Dq groups. **(D).** Representative (left) and average (right) traces of mIPSCs recorded from CtrL+GFP (blue), Sus+GFP (orange) and Sus+hM3Dq (red) mouse mPFC PNs. **(E and F).** Cumulative probability of mIPSC inter-event interval (Left) and amplitude (Right) in CtrL+GFP (blue, n = 35 cells from 3 mice), Sus+GFP (orange, n = 30 cells from 3 mice) and Sus+hM3Dq (red, n = 25 cells from 3 mice) groups. Insets: average mIPSC frequency and amplitude from CtrL+GFP, Sus+GFP and Sus+hM3Dq groups. **(G).** Representative traces of evoked EPSC and IPSC in same mPFC PNs from CtrL+GFP, Sus+GFP and Sus+hM3Dq groups. **(H and I).** The maximal EPSC (H) and IPSC (I) recorded from CtrL+GFP (blue, n = 33 cells from 3 mice), Sus+GFP (orange, n = 28 cells from 3 mice) and Sus+hM3Dq (red, n = 32 cells from 3 mice) groups. **(J).** The calculated E/I ratio from CtrL+GFP, Sus+GFP and Sus+hM3Dq groups. mPFC, medial prefrontal cortex; MD, mediodorsal thalamus; Ctrl, control; Sus, susceptible. PN, pyramidal neurons. Ctrl+GFP: Control mice that received MD injection of AAV-CaMKIIα-EGFP and CNO bath applications (10μM); Sus+GFP: Sus mice that received MD injection of AAV-CaMKIIα-EGFP and CNO bath applications (10μM); Sus+hM3Dq: Sus mice that received MD injection of AAV-CaMKIIα-hM3Dq-EGFP and CNO bath applications (10μM). *$P < 0.05$, **$p < 0.01$, ***$p < 0.001$, One-way ANOVA test; Data represents mean±SEM.

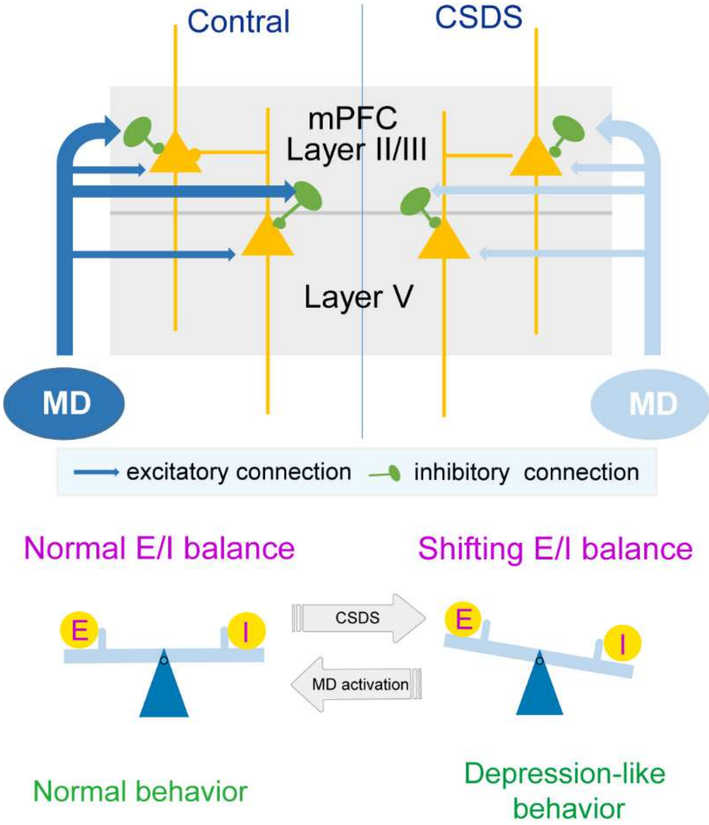


**Figure 8. MD modulates mPFC PNs E/I balance to influence depression-like behavior.**

Under normal conditions, the MD provides a glutamatergic projection to mPFC layers II/III and V and has stronger input to interneurons than pyramidal neurons. This also implies that mPFC PNs maintain a high level of inhibition in the MD-mPFC circuit. In depressed mice, MD to mPFC connectivity is reduced, leading to disinhibition of mPFC PNs, resulting in increased mPFC PNs excitability and altered E/I balance. Yellow triangles and green circles represent pyramidal neurons (PNs) and interneurons in the mPFC, respectively. Blue ovals represent MD neurons. Dark blue represents high levels of activity, while light blue represents decreased activity. This pattern map is based on our findings and known MD predictions of mPFC connectivity (19).

## References

1. Mathers CD, Loncar D. Projections of global mortality and burden of disease from 2002 to 2030. PLoS Med. 2006;3(11):e442.

2. Gotlib IH, Joormann J. Cognition and depression: current status and future directions. Annu Rev Clin Psychol. 2010;6:285-312.

3. <Depression.pdf>.

4. Tanti A, Belzung C. Open questions in current models of antidepressant action. Br J Pharmacol. 2010;159(6):1187-200.

5. Shepherd GM. Corticostriatal connectivity and its role in disease. Nat Rev Neurosci. 2013;14(4):278-91.

6. Bora E, Harrison BJ, Davey CG, Yucel M, Pantelis C. Meta-analysis of volumetric abnormalities in cortico-striatal-pallidal-thalamic circuits in major depressive disorder. Psychol Med. 2012;42(4):671-81.

7. Greicius MD, Flores BH, Menon V, Glover GH, Solvason HB, Kenna H, et al. Resting-state functional connectivity in major depression: abnormally increased contributions from subgenual cingulate cortex and thalamus. Biol Psychiatry. 2007;62(5):429-37.

8. Lui S, Wu Q, Qiu L, Yang X, Kuang W, Chan RC, et al. Resting-state functional connectivity in treatment-resistant depression. Am J Psychiatry. 2011;168(6):642-8.

9. Sherman SM, Guillery RW. Functional organization of thalamocortical relays. J Neurophysiol. 1996;76(3):1367-95.

10. Guillery RW. Anatomical evidence concerning the role of the thalamus in corticocortical communication: a brief review. J Anat. 1995;187 ( Pt 3):583-92.

11. Brown EC, Clark DL, Hassel S, MacQueen G, Ramasubbu R. Intrinsic thalamocortical connectivity varies in the age of onset subtypes in major depressive disorder. Neuropsychiatr Dis Treat. 2019;15:75-82.

12. Haber SN. The primate basal ganglia: parallel and integrative networks. J Chem Neuroanat. 2003;26(4):317-30.

13. Mitchell AS. The mediodorsal thalamus as a higher order thalamic relay nucleus important for learning and decision-making. Neurosci Biobehav Rev. 2015;54:76-88.

14. De Witte L, Brouns R, Kavadias D, Engelborghs S, De Deyn PP, Marien P. Cognitive, affective and behavioural disturbances following vascular thalamic lesions: a review. Cortex. 2011;47(3):273-319.

15. Van der Werf YD, Scheltens P, Lindeboom J, Witter MP, Uylings HB, Jolles J. Deficits of memory, executive functioning and attention following infarction in the thalamus; a study of 22 cases with localised lesions. Neuropsychologia. 2003;41(10):1330-44.

16. Groenewegen HJ. Organization of the afferent connections of the mediodorsal thalamic nucleus in the rat, related to the mediodorsal-prefrontal topography. Neuroscience. 1988;24(2):379-431.

17. Parnaudeau S, Bolkan SS, Kellendonk C. The Mediodorsal Thalamus: An Essential Partner of the Prefrontal Cortex for Cognition. Biol Psychiatry. 2018;83(8):648-56.

18. Giraldo-Chica M, Rogers BP, Damon SM, Landman BA, Woodward ND. Prefrontal-Thalamic Anatomical Connectivity and Executive Cognitive Function in Schizophrenia. Biol Psychiatry. 2018;83(6):509-17.

19. Ferguson BR, Gao WJ. Thalamic Control of Cognition and Social Behavior Via Regulation of Gamma-Aminobutyric Acidergic Signaling and Excitation/Inhibition Balance in the Medial Prefrontal Cortex. Biol Psychiatry. 2018;83(8):657-69.

20. Hammen C. Stress and depression. Annu Rev Clin Psychol. 2005;1:293-319.

21. Mouri A, Ukai M, Uchida M, Hasegawa S, Taniguchi M, Ito T, et al. Juvenile social defeat stress exposure persistently impairs social behaviors and neurogenesis. Neuropharmacology. 2018;133:23-37.

22. Hauenstein EJ. Depression in adolescence. J Obstet Gynecol Neonatal Nurs. 2003;32(2):239-48.

23. Ray JP, Price JL. The organization of projections from the mediodorsal nucleus of the thalamus to orbital and medial prefrontal cortex in macaque monkeys. J Comp Neurol. 1993;337(1):1-31.

24. Bolkan SS, Stujenske JM, Parnaudeau S, Spellman TJ, Rauffenbart C, Abbas AI,

et al. Publisher Correction: Thalamic projections sustain prefrontal activity during working memory maintenance. Nat Neurosci. 2018;21(8):1138.

25. Mitchell AS. The mediodorsal thalamus as a higher order thalamic relay nucleus important for learning and decision-making. Neurosci Biobehav R. 2015;54:76-88.

26. Sherman SM, Guillery RW. Distinct functions for direct and transthalamic corticocortical connections. J Neurophysiol. 2011;106(3):1068-77.

27. Rovo Z, Ulbert I, Acsady L. Drivers of the primate thalamus. J Neurosci. 2012;32(49):17894-908.

28. Lee S, Shin H-S. The role of mediodorsal thalamic nucleus in fear extinction. Journal of Analytical Science and Technology. 2016;7(1).

29. Cardoso EF, Maia FM, Fregni F, Myczkowski ML, Melo LM, Sato JR, et al. Depression in Parkinson's disease: convergence from voxel-based morphometry and functional magnetic resonance imaging in the limbic thalamus. Neuroimage. 2009;47(2):467-72.

30. Zhu X, Tang HD, Dong WY, Kang F, Liu A, Mao Y, et al. Distinct thalamocortical circuits underlie allodynia induced by tissue injury and by depression-like states. Nat Neurosci. 2021;24(4):542-53.

31. Huang L, Xi Y, Peng Y, Yang Y, Huang X, Fu Y, et al. A Visual Circuit Related to Habenula Underlies the Antidepressive Effects of Light Therapy. Neuron. 2019;102(1):128-42 e8.

32. Dwyer JM, Maldonado-Aviles JG, Lepack AE, DiLeone RJ, Duman RS. Ribosomal protein S6 kinase 1 signaling in prefrontal cortex controls depressive behavior. Proc Natl Acad Sci U S A. 2015;112(19):6188-93.

33. Krishnan V, Nestler EJ. Linking molecules to mood: new insight into the biology of depression. Am J Psychiatry. 2010;167(11):1305-20.

34. Jiang B, Wang W, Wang F, Hu ZL, Xiao JL, Yang S, et al. The stability of NR2B in the nucleus accumbens controls behavioral and synaptic adaptations to chronic stress. Biol Psychiatry. 2013;74(2):145-55.

35. Arnsten AF. Stress signalling pathways that impair prefrontal cortex structure and function. Nat Rev Neurosci. 2009;10(6):410-22.

36. Arnsten AF. Stress weakens prefrontal networks: molecular insults to higher cognition. Nat Neurosci. 2015;18(10):1376-85.

37. Cho JH, Deisseroth K, Bolshakov VY. Synaptic encoding of fear extinction in mPFC-amygdala circuits. Neuron. 2013;80(6):1491-507.

38. Lee AT, Cunniff MM, See JZ, Wilke SA, Luongo FJ, Ellwood IT, et al. VIP Interneurons Contribute to Avoidance Behavior by Regulating Information Flow across Hippocampal-Prefrontal Networks. Neuron. 2019;102(6):1223-34 e4.

39. Fan Z, Hu H. Medial Prefrontal Cortex Excitation/Inhibition Balance and Schizophrenia-like Behaviors Regulated by Thalamic Inputs to Interneurons. Biol Psychiatry. 2018;83(8):630-1.

40. Yizhar O, Fenno LE, Prigge M, Schneider F, Davidson TJ, O'Shea DJ, et al. Neocortical excitation/inhibition balance in information processing and social dysfunction. Nature. 2011;477(7363):171-8.

41. Selimbeyoglu A, Kim CK, Inoue M, Lee SY, Hong ASO, Kauvar I, et al. Modulation of prefrontal cortex excitation/inhibition balance rescues social behavior in CNTNAP2-deficient mice. Sci Transl Med. 2017;9(401).

42. Dong Z, Chen W, Chen C, Wang H, Cui W, Tan Z, et al. CUL3 Deficiency Causes Social Deficits and Anxiety-like Behaviors by Impairing Excitation-Inhibition Balance through the Promotion of Cap-Dependent Translation. Neuron. 2020;105(3):475-90 e6.

43. Coghlan S, Horder J, Inkster B, Mendez MA, Murphy DG, Nutt DJ. GABA system dysfunction in autism and related disorders: from synapse to symptoms. Neurosci Biobehav Rev. 2012;36(9):2044-55.

44. Nelson SB, Valakh V. Excitatory/Inhibitory Balance and Circuit Homeostasis in Autism Spectrum Disorders. Neuron. 2015;87(4):684-98.

45. Yoon T, Okada J, Jung MW, Kim JJ. Prefrontal cortex and hippocampus subserve different components of working memory in rats. Learn Mem. 2008;15(3):97-105.

46. Golden SA, Covington HE, 3rd, Berton O, Russo SJ. A standardized protocol for repeated social defeat stress in mice. Nat Protoc. 2011;6(8):1183-91.

47. He F, Zhang P, Zhang Q, Qi G, Cai H, Li T, et al. Dopaminergic Projection from Ventral Tegmental Area to Substantia Nigra Pars Reticulata Mediates Chronic Social

Defeat Stress-Induced Hypolocomotion. Mol Neurobiol. 2021;58(11):5635-48.
48. Can A, Dao DT, Terrillion CE, Piantadosi SC, Bhat S, Gould TD. The tail suspension test. J Vis Exp. 2012(59):e3769.
49. Yan S, You ZL, Zhao QY, Peng C, He G, Gou XJ, et al. Antidepressant-like effects of Sanyuansan in the mouse forced swim test, tail suspension test, and chronic mild stress model. Kaohsiung J Med Sci. 2015;31(12):605-12.

**Acknowledgements**

This work was supported by the National Natural Science Foundation of China (81771144, 81571191). Natural Science Foundation of Guangdong Province, China (2021A1515011134, 2017B030311002). GuangDong Basic and Applied Basic Research Foundation (81571191). Fundamental Research Funds for the Central Universities (11620325). The Research Foundation of Medical Science and Technology of Guangdong Province (A2022262).

**Author contributions**

G-GQ, LF and Z-JF carried out the study conceptualization and experimental design. LF performed whole-cell patch-clamp recordings, behavioral tests, Virus injection, formal analysis and wrote the manuscript; WHJ and M-LH performed behavioral tests, Virus injection, behavioral analysis and investigation. C-MY performed Microscopy imaging and immunofluorescence. H-YQ and L-DL performed brain perfusion, L-YF and X-KM performed electrophysiological statistics; G-GQ, Z-JF and Z-XF performed fund acquisition and topic discussion. All the authors read and approved this manuscript.

We appreciate technical support by Dr. Bin Jiang in Zhongshan school of medicine, SYSU.

**Competing interests**

The authors declare no competing interests.

# Supplementary Files

This is a list of supplementary files associated with this preprint. Click to download.

- SupplementaryInformation.pdf